Mechanical Technology and Engineering Insights

www.mtei.reapress.com

Mech. Technol. Eng. Insights. Vol. 3, No. 1 (2026) 101–117.

Paper Type: Original Article

Numerical Investigation of the Effect of Artificial Roughness on the Flow Field and Heat Transfer Rate in a Rectangular Channel

Hamed Mohaddes Deylami[1,*], Soheila Sojodi[1]

[1] Department of Mechanical Engineering, University of Guilan, Rasht, Iran; hmohaddesd@gmail.com; soheila_sojodi@yahoo.com.

Citation:

Received: 16 October 2025 *Revised: 21 Desember 2025* *Accepted: 14 February 2026*	Mohaddes Deylami, H., & Sojodi, S. (2026). Numerical investigation of the effect of artificial roughness on the flow field and heat transfer rate in a rectangular channel. *Mechanical Technology and Engineering Insights, 3*(2), 101-117.

Abstract

In the current study, the numerical analysis of the turbulent flow field and heat transfer in a flat rectangular channel having roughness elements on its bottom surface is conducted. Two dimensional, steady, incompressible and turbulent flow simulations are carried out using the Finite Volume Method (FVM). In this regard, the structured non-uniform quadrilateral mesh is chosen, where the pressure term is discretized using the standard scheme while all other governing equations are discretized by using second order upwind scheme. The SIMPLE scheme is used for coupling the pressure velocity field. The effect of important parameters such as Reynolds number ($5400 < Re < 23000$), ratio of roughness height to channel height ($0.06 < e/H < 0.26$) and ratio of roughness thickness to pitch ($0.25 < t/P < 1.0$) on average Nusselt number, friction factor and thermal performance improvement factor has been investigated. It is found that increase in Reynolds number increases the heat transfer rate but decreases the thermal performance factor. Moreover, increase in ratio of thickness to pitch and decrease in ratio of height to channel improves the thermal performance. The RNG k ε turbulence model shows better prediction compared to the experimental data.

Keywords: Artificial roughness, Heat transfer enhancement, Numerical investigation, Rectangular channel, Turbulent flow, RNG k-ε model, Thermal performance factor.

1 | Introduction

The growing global demand for high-efficiency heat transfer systems with lower energy consumption has made the improvement of thermal performance of heat transfer equipment one of the most important research areas in mechanical and energy engineering. Heat exchangers, gas turbine cooling channels, heat recovery systems, electronic systems, chemical reactors, and solar collectors are only a part of the equipment

Corresponding Author: hmohaddesd@gmail.com

https://doi.org/10.48313/mtei.v3i2.83

Licensee System Analytics. This article is an open access article distributed under the terms and conditions of the Creative Commons Attribution (CC BY) license (http://creativecommons.org/licenses/by/4.0).

whose performance is strongly influenced by the convective heat transfer rate. Increasing the heat transfer rate in flow channels plays a key role in the optimal design of compact heat exchangers, advanced cooling systems in the electronics industry, and energy recuperators in aerospace and automotive industries [1].

Despite their widespread applicability, smooth surfaces in channels have an inherent limitation in heat transfer due to the formation of a thick thermal boundary layer, which has driven researchers toward employing heat transfer enhancement methods [2]. Among the various methods, passive techniques such as artificial roughness, turbulators, and corrugated plates have received special attention in studies because they do not require external power consumption [3]. Although the use of artificial roughness, by disrupting the boundary layer and increasing turbulence intensity, leads to a noticeable improvement in heat transfer, it is simultaneously accompanied by an increase in frictional pressure drop, which makes the simultaneous evaluation of the thermal performance enhancement criterion an unavoidable necessity [4]. Despite the numerous studies on corrugated and wavy channels with continuous geometries, the combined effect of independent geometrical parameters of discrete roughness elements (including the height ratio and thickness-to-pitch ratio) on the flow field and heat transfer in rectangular channels with constant cross-section has been less systematically investigated over a wide range of turbulent Reynolds numbers.

Therefore, the main objective of the present study is the numerical investigation of the combined effect of these geometrical parameters on the thermal and hydraulic performance of turbulent flow in a rectangular channel with artificial roughness on the bottom surface. In general, the broad spectrum of research conducted in the field of corrugated and roughened channels can be divided into two main categories: Experimental investigations and numerical simulations. However, since in many of these studies experimental and numerical approaches have been carried out simultaneously, the separation of these two areas has been avoided.The problem of viscous flow in a wavy channel was first analytically studied by Burns and Parks [5], who stated that the stream function, assuming Stokes flow, can be expressed as a Fourier series.

Goldstein and Sparrow [6] were the first to use the naphthalene sublimation method to measure local and average heat transfer coefficients in a triangular wavy channel. Their experiments were conducted for laminar, transitional, and turbulent flows at two wavelengths. Comparison of their results with those obtained for flow between parallel smooth plates showed that the average heat transfer in turbulent flow in this case increased by 3 times.

Also, O'Brien and Sparrow [7] performed a comprehensive study on the same geometry with more wavelengths. The results showed that the heat transfer enhancement in this case was 2.5 times that of smooth channels in the fully developed state.

In 1993, Saniei and Dini [8] experimentally investigated the heat transfer characteristics in a turbulent regime for a wavy channel. They concluded that the highest local Nusselt number occurs at the crest of each wave, while the lowest local Nusselt number is located a short distance downstream of the crest. They also found that in a fully developed flow, the highest average Nusselt number belongs to the second wave, and the Nusselt number remains approximately constant from the third wave onward.

Wang and Vanka [9] obtained the heat transfer rate for flow in regularly wavy channels. They found that in steady flow, the average Nusselt number in the wavy channel is slightly larger than that in the smooth-plate channel. However, in transitional flow, heat transfer in the wavy channel is 2.5 times that of the smooth channel. Also, the friction factor for the wavy channel is about 2 times that of the smooth channel in steady flow, and this value remains approximately constant in the transitional regime.

Patel et al. [10] using direct numerical solution of the Navier–Stokes equations and a linear turbulence model, obtained velocity profiles and Reynolds stresses and compared their numerical results with experimental data. In that study, it was shown that the employed turbulence model could adequately predict the flow separation and reattachment points.

Gloerfelt and Cinnella [11] using Large Eddy Simulation (LES), investigated turbulent flow in a channel with a smooth upper wall and a wavy lower wall. The computations were performed at a Reynolds number of

60000 based on the wave height and the maximum velocity at the channel centre. Using this method, they showed that the locations of separation and reattachment points are highly dependent on the computational grid. Ziefle et al. [12] also used LES to compare velocities and Reynolds stresses with experimental values. Their results indicated that the differences between the predictions of this method and experimental data were very smal.

A numerical and experimental study on the transitional characteristics of flow regime and heat transfer in fully developed flow inside a corrugated channel was conducted by Yang et al. [13]. Measurements were performed for Reynolds numbers between 100 and 2500 on a triangular corrugated channel with vane angles of 15° and 30°. They found that the transitional Reynolds number from laminar to turbulent flow in the corrugated channel is lower than that in the smooth channel, and this value decreases with increasing vane angle. The transitional Reynolds number for a vane angle of 30° was about 700.

Amano [14], in a numerical study, investigated laminar and turbulent flows in the Reynolds number range of 10 to 25000 in periodically corrugated channels. He used the standard turbulence model for numerical modelling and found that the heat transfer and surface friction patterns change dramatically from laminar to turbulent flow.

Islamoglu and Parmaksizoglu [15], [16] experimentally examined the effect of channel height (the distance between the lower and upper plates) on heat transfer enhancement in a corrugated-plate heat exchanger and confirmed the accuracy of their experimental results numerically. Their experiments were carried out for two different channel heights of 5 and 10 mm and a vane angle of 20° in the Reynolds number range of 1200 to 4000. They revealed that with increasing channel height, the average Nusselt number increases simultaneously with pressure drop. Naphon and co-workers [17–19] experimentally and numerically investigated heat transfer for laminar and turbulent flows in single-sided and double-sided corrugated channels, with various vane angles and channel heights, with the ribs arranged in-line and with phase shift, under constant heat flux boundary conditions, using the standard turbulence model. The results obtained from their investigations showed that, in general, the corrugated plate has a significant effect on increasing heat transfer in the channel, and consequently, the use of corrugated plates is a suitable method for improving thermal performance and thus making heat exchangers smaller and more compact.

Eiamsa-ard and Promvonge [20], in their numerical study on the effect of the groove depth-to-channel height ratio (B/H) on heat transfer and pressure drop for Reynolds numbers between 6000 and 18000 in periodically corrugated channels with rectangular grooves, examined four turbulence models: Standard, RNG, standard, and SST to find the best model. They found that the standard and RNG models showed better agreement with available experimental data. Also, a significant increase in heat transfer was observed in the corrugated channel with rectangular grooves compared to the smooth channel.

Thianpong et al. [21] conducted an experimental study to investigate the effects of rib height, rib arrangement, and Reynolds number on heat transfer and pressure drop in a corrugated channel with isosceles triangular ribs, over the Reynolds number range of 5000 to 23000. They revealed that the rib arrangement with a phase shift of 0° results in higher heat transfer and, at the same time, higher pressure drop than the arrangement with a phase shift of 180°. They also found that increasing the rib height simultaneously increases the friction factor and the Nusselt number.

Elshafei et al. [22], in an experimental study, investigated heat transfer and pressure drop in corrugated channels with triangular ribs under constant and uniform wall temperature, for various distances and phase shifts between the channel plates, in the Reynolds number range of 3220 to 9420. Their results showed that at high Reynolds numbers, changes in the distances between the channel plates have a greater effect on pressure drop than changes in the phase shift. The effect of phase shift between the upper and lower channel plates on the flow pattern and heat transfer characteristics in a wavy channel with sinusoidal protrusions under constant wall temperature was numerically studied by Yin et al. [23]. Their results showed that in the

investigated Reynolds number range of 2000 to 10000, the phase-shift effect is more pronounced at higher Reynolds numbers, while a zero-degree phase shift gives better performance at lower Reynolds numbers.

Tanda [24] conducted an experimental study on the thermal performance of a corrugated channel with inclined rectangular ribs at an angle of 45° in the spanwise direction. The rib height-to-hydraulic diameter ratio (e/D) was 0.09 and the pitch-to-height ratio (p/e) was set to different values of 6.66, 10, 13.33, and 20. His results showed that the optimum heat transfer performance occurs at a pitch-to-height ratio of 13.33 for the channel with corrugated plate on one side, and at a pitch-to-height ratio of 6.66 to 10 for the channel with corrugated plates on both sides.

The effect of Reynolds number on flow instability and also the effect of changing the oscillation amplitude in a sinusoidal wavy channel were numerically investigated by Ramgadia and Saha [25]. They studied different geometries with various ratios of minimum to maximum distance between channel plates (Hmin/Hmax) from 0.1 to 0.5 and found that Hmin/Hmax = 0.2 provides the highest Nusselt number and the best thermal performance factor in the channel. They also revealed that the critical Reynolds number regarding system instability is highly dependent on the channel geometrical parameters.A three-dimensional numerical investigation of heat transfer and pressure drop in a corrugated channel with rectangular ribs for Reynolds numbers between 75 and 2000 was performed by Desrues et al. [26]. They found that heat transfer in the corrugated channel increases relative to the flat channel only when the Reynolds number exceeds a certain value, and that specific value also depends on the channel geometrical parameters.

Mohammed et al. [27] performed a numerical analysis of the experimental study of Naphon [19] using the standard turbulence model. They investigated the problem for a wider range of Reynolds numbers and phase shifts and confirmed that the use of corrugated channels is an appropriate method to increase the efficiency of heat exchangers. In addition, recent research has shown that the type of roughness geometry and its arrangement play a decisive role in the formation of vortices and flow reattachment regions [28].

Accordingly, the present study aims at the numerical investigation of turbulent flow and heat transfer in a rectangular channel equipped with artificial roughness. In this study, the effects of Reynolds number, roughness height-to-channel height ratio, and roughness thickness-to-pitch ratio on the flow field, average Nusselt number, friction factor, and thermal performance enhancement factor have been evaluated. The simulations are carried out using the Finite Volume Method (FVM) and solving the governing equations for steady, two-dimensional, incompressible flow. The results of this research can be used in the optimal design of heat transfer channels and compact heat exchangers, with the goal of achieving maximum heat transfer along with minimum pressure drop, and can provide a suitable perspective for selecting roughness geometrical parameters in engineering applications.

2 | Numerical Methodology

In the present study, the Computational Fluid Dynamics (CFD) approach is employed to simulate the turbulent flow and heat transfer in flat channels equipped with artificial roughness. This section provides a detailed description of the numerical solution procedure, including the computational domain, mesh generation and quality assessment, grid independence verification, governing equations for flow and temperature fields, turbulence modeling, boundary conditions, and the discretization and solution methods.

2.1 | Computational Domain and Boundary Conditions

A schematic view of the problem geometry is shown in *Fig. 1*. To ensure fully developed flow at the inlet of the roughened section and to eliminate the effects of outlet boundary conditions on the upstream flow field, an upstream length of 20 times the channel height (20H) and a downstream length of 10 times the channel height (10H) are considered. The detailed geometrical parameters, including the total channel length, height, roughness dimensions, and pitch, are summarized in *Table 1*.

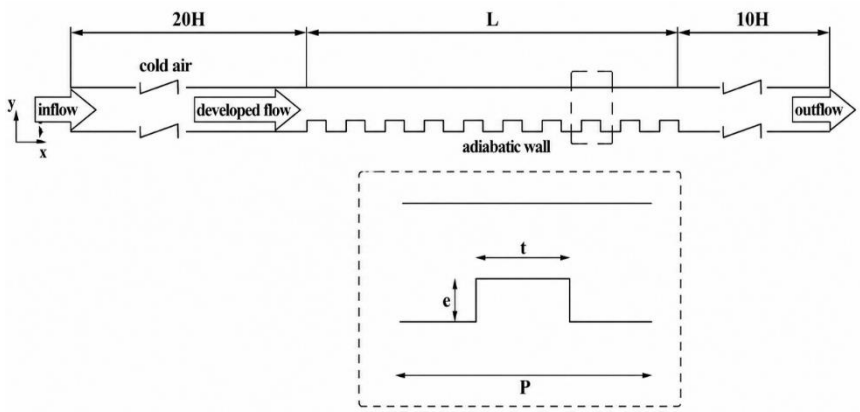

Fig. 1. Schematic view of the problem geometry.

Table 1. Geometrical parameters used in the simulations.

Value (mm)	Parameter
950	Total channel length
15	Channel height, H
500	Test section length, L
300	Upstream length
150	Downstream length
1, 2, 3, 4	Roughness height, e
0, 10, 20, 30, 40	Roughness thickness, t
40	Roughness pitch, P

The applied boundary conditions are as follows: At the inlet, a uniform velocity profile and a constant temperature (ambient temperature) are specified. At the outlet, a zero-gauge-pressure condition (fully developed outflow) is imposed. The upper wall of the channel is assumed adiabatic (zero heat flux), while the bottom wall (where the roughness elements are placed) is subjected to a constant heat flux. Additionally, the no-slip condition is applied on all solid walls.

2.2 | Governing Equations for Turbulent Flow

The flow is assumed to be two-dimensional, incompressible, turbulent, and steady. The governing equations, namely continuity, momentum, and energy, are presented here in their Reynolds-Averaged (RANS) form.

2.2.1 | Continuity equation

$$\frac{\partial \overline{u_i}}{\partial x_i} = 0. \tag{1}$$

After Reynolds time-averaging, the continuity equation for the mean flow retains the same form as *Eq. (1)*, since the spatial derivative of the fluctuating velocity components vanishes for incompressible flow.

The momentum equation for a turbulent, incompressible flow with constant properties is written as:

$$\rho\left(\frac{\partial \overline{u_i}}{\partial t} + \overline{u_j}\frac{\partial \overline{u_i}}{\partial x_j} + \overline{u_j{}'\frac{\partial u_i{}'}{\partial x_j}}\right) = \overline{B_i} - \frac{\partial \overline{p}}{\partial x_i} + \frac{\partial}{\partial x_j}\left(\mu\frac{\partial \overline{u_i}}{\partial x_j} - \rho\overline{u_i{}'u_j{}'}\right), \tag{2}$$

where $\overline{u_i}$ and p are the time-averaged velocity components and pressure, respectively. The term $\rho\overline{u_i'u_j'}$ arises from the averaging process and is known as the Reynolds stress tensor. Physically, this term represents the additional momentum exchange due to turbulent fluctuations and acts as an apparent stress on the mean flow. The presence of this unknown term renders the governing equations unclosed (the closure problem of turbulence), necessitating the use of turbulence models.To close the RANS equations and compute the Reynolds stresses, standard two-equation turbulence models are employed (the chosen model is validated

against available experimental data in the Results section). The energy equation is also solved in its RANS form, accounting for the turbulent heat flux term $\varrho C_p \overline{u_i' T}$.

The computational mesh consists of a structured (organized), non-uniform grid with quadrilateral elements (for the 2D domain). Due to the steep velocity and temperature gradients near the walls and around the roughness edges, local grid refinement is applied in these regions. The discretization of the governing equations is performed using the FVM. Specifically, the pressure term is discretized using the standard scheme, while the convective and diffusive terms are treated with a second-order upwind approximation. The pressure-velocity coupling is handled by the SIMPLE algorithm.

To evaluate the hydraulic and thermal performance of the channel, the following dimensionless parameters are defined: The local and average Nusselt numbers are obtained respectively from:

$$Nu_x = \frac{h_x D_h}{K}. \quad (3)$$

$$\overline{Nu} = \frac{\overline{h} D_h}{K}. \quad (4)$$

All thermophysical properties of air (density, dynamic viscosity, thermal conductivity, and specific heat) are evaluated at the mean bulk temperature (T_b) to ensure accuracy of the calculations. The numerical results are validated by comparison with experimental data available in the literature [29], [30] confirming the correctness of the solution procedure and the adequacy of the selected turbulence model.

2.3 | Mesh Generation

Computational mesh generation is one of the most sensitive and influential steps in any numerical simulation. In the present study, mesh generation is carried out using the commercial software Gambit 2.4.6. The procedure involves defining vertices, edges, and faces of the computational domain, followed by mesh generation on the domain, and subsequent assignment of boundary conditions to the relevant faces. The prepared mesh is then exported to the Fluent solver.

Given the two-dimensional nature of the problem, quadrilateral cells are employed for discretization. A schematic view of the mesh arrangement around a roughness element is shown in *Fig. 2*.

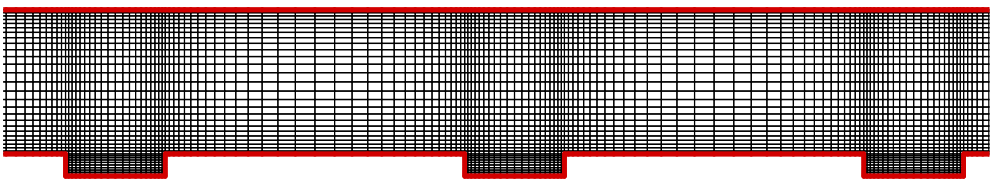

Fig. 2. Schematic view of the computational mesh arrangement around the artificial roughness.

To enhance numerical accuracy in the near-wall region, the dimensionless wall distance (y+) is maintained below 5 and, wherever possible, close to unity. This range is well suited for employing the "enhanced wall treatment," which will be described in the section on wall functions, and allows accurate resolution of the steep velocity and temperature gradients within the boundary layer.

3 | Numerical Solution Procedure and Discretization

The governing equations, namely the two-dimensional, steady, incompressible continuity, momentum, energy, and the RNG k−εturbulence model equations–are discretized using the FVM. The solver is pressure-based, which is highly efficient for incompressible flows.

The discretization schemes are selected as follows:

I. Pressure term: Standard scheme.

II. Other convective and diffusive terms: Second-order upwind approximation.

The pressure-velocity coupling is handled via the SIMPLE algorithm. This algorithm relates the velocity components on cell faces to the pressure field through the discretized momentum equations and derives the pressure-correction equation from the continuity equation.

3.1 | Convergence

To enhance numerical stability and achieve satisfactory convergence, the under-relaxation factors for the momentum, Turbulent Kinetic Energy (TKE), and turbulent dissipation rate (εε) equations are reduced to 0.5, while that for the pressure equation is set to 0.3. Convergence is considered achieved when the following three conditions are simultaneously satisfied:

I. The scaled residuals of all equations drop to at least 10^{-7}.

II. The net mass imbalance across the channel is reduced to less than 0.2% of the total mass flow rate.

III. Important integral quantities such as velocity and temperature at sensitive locations show no significant changes over successive iterations.

A sample residual reduction history is presented in *Fig. 3*.

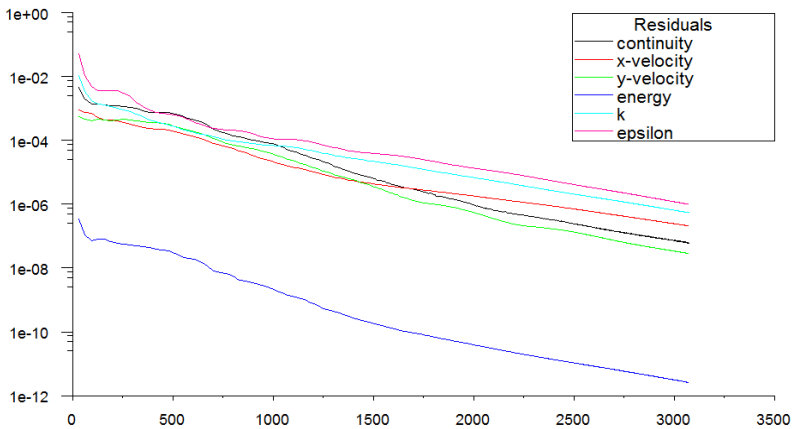

Fig. 3. Sample residual reduction history for the present simulations.

All computations are performed on an Intel Core i5 2.53 GHz processor using parallel processing. The computational time per case ranges from 3 to 5 hours, depending on the geometric complexity and the number of mesh cells.

4 | Result and Discussion

Given the trade-offs between accuracy, computational cost, and hardware limitations, a two-equation turbulence model was preferred for this study. To identify the most suitable variant, four two-equation models were evaluated using the Enhanced Wall Treatment, and their predictions were compared with the experimental data of Thianpong et al. [21] for a geometry with e/H=0.26, t/P=0.5, and z/t=0.

As shown in *Fig. 4*, the RNG k−ε model exhibits the closest agreement with the experimental results for both the friction factor and the average Nusselt number across the examined Reynolds number range. Therefore, the RNG k−ε model was selected for all subsequent simulations.

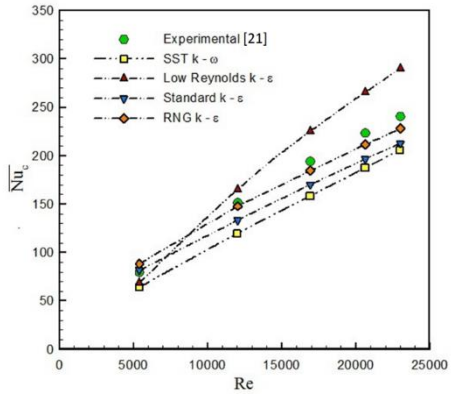

a.

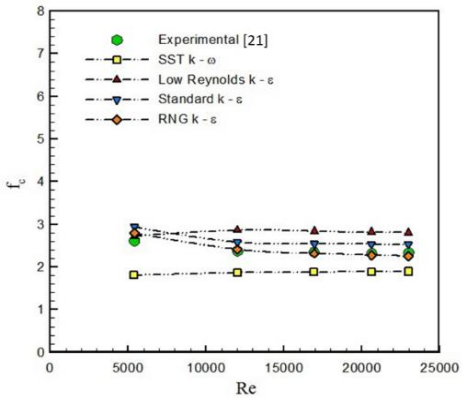

b.

Fig. 4. Comparison of numerical results for different turbulence models with the experimental data of Thianpong et al. [21] for various Reynolds numbers; a. friction factor, b. average Nusselt number.

4.1|Effect of Roughness Thickness-to-Pitch Ratio (t/P)

The effect of the roughness thickness to pitch ratio (t/P) on the hydraulic and thermal characteristics of the channel is examined in this part of the study. Numerical simulation is conducted for four different values of t/P, i.e., 0.25, 0.50, 0.75, and 1.00 over Reynolds number ranging from 5400 to 23000. The results are shown and discussed in terms of friction factor, Nusselt number, temperature distribution, TKE, and thermal performance enhancement factor. *Fig. 5* shows the variation of the friction factor for the roughened channel (f) and the ratio between the friction factors of the roughened and smooth channels (f/f0) with Reynolds number for various t/P ratios. It is noted that the friction factor of the roughened channel increases marginally with Reynolds number, while the ratio f/f0 decreases. In addition, an increase in t/P results in a decrease in both the above quantities, with the largest value of friction factor for t/P=0.25 and the smallest for t/P=1.00. This decrease is due to the decreased cavity length and hence less recirculation zones near the roughness elements.

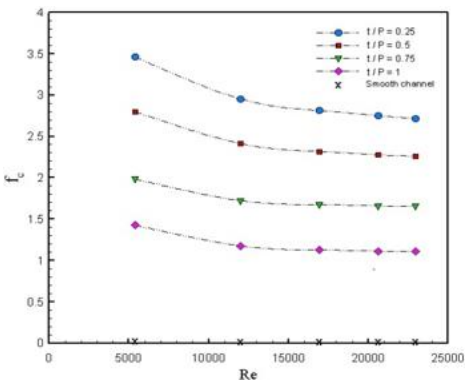

a.

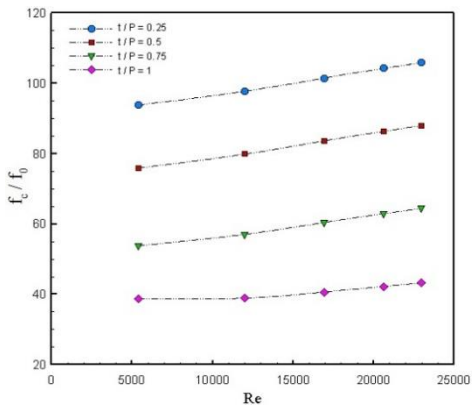

b.

Fig. 5. Variation with Reynolds number for different t/P ratios; a. friction factor in the roughened channel, b. ratio of friction factor in the roughened channel to that of the smooth channel.

Fig. 6 shows a comparison of the streamlines at Re=16920 for t/P=0.25 and t/P=0.75. The introduction of the roughness leads to a flow separation and the creation of the recirculation areas within the cavities. In case of t/P=0.25, the recirculation zones become larger with the appearance of clearly visible vortices behind the roughness obstacles. With the increase of t/P up to 0.75, the sizes of the recirculation zones become smaller, and the flow is able to move over the roughness without large efforts. Such changes in the flow structure are among the major parameters affecting both friction factor and heat transfer.

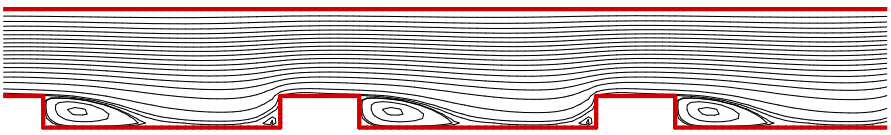

a.

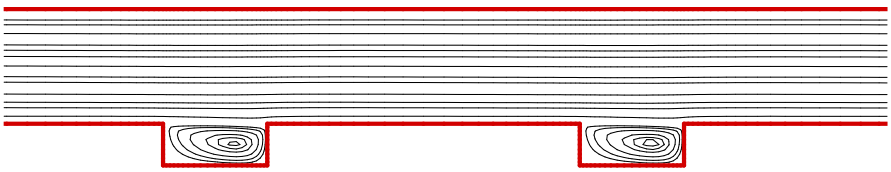

b.

Fig. 6. Streamlines at Re=16920; a. t/P=0.25, b. t/P=0.75.

Fig. 7 demonstrates the distribution of the TKE at Re=16920 for t/P=0.25 and t/P=0.75. The maximums of TKE are achieved around the roughness obstacles within the separated and reattachment areas. In case of t/P=0.25, due to the presence of more extensive recirculation zones, the higher intensities of TKE are achieved near the rough surface. With the increasing value of t/P, the flow structure and, correspondingly, the distribution of the TKE become significantly different. These differences influence the fluid mixing and, therefore, the convective heat transfer from the heated wall to the main flow.

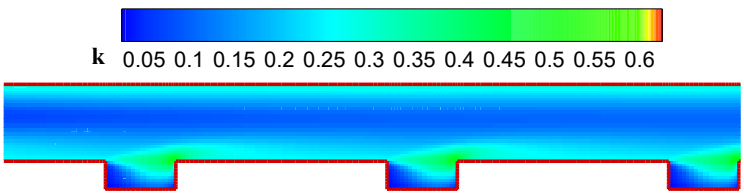

a.

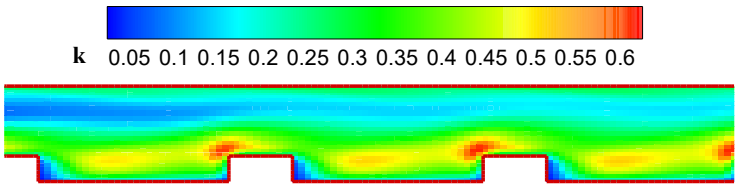

b.

Fig. 7. TKE distribution at Re=16920, a. t/P=0.25, b. t/P=0.75.

Fig. 8 depicts the dependence of the average Nusselt number and the ratio of this Nusselt number to the smooth channel's one (Nu/Nu0) on the Reynolds number for different values of the t/P ratio. The average Nusselt number increases with increasing Reynolds number, which means that the heat transfer is more intensive at higher Reynolds numbers. On the other hand, the Nu/Nu0 ratio decreases with increasing Reynolds number, which means that even though the heat transfer rate increases with Reynolds number, the relative gain over the smooth channel decreases with Reynolds number. At a fixed value of Reynolds number, the Nusselt number first increases with increasing t/P ratio until it attains a maximum at t/P = 0.50, then it falls as t/P continues to increase.

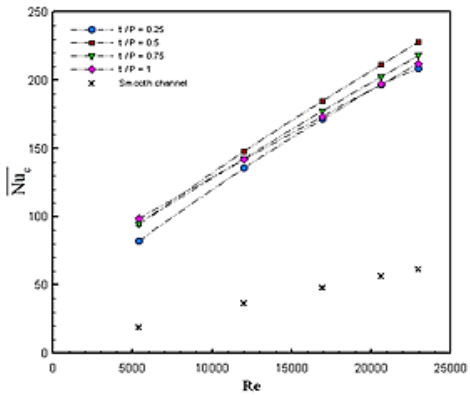

a.

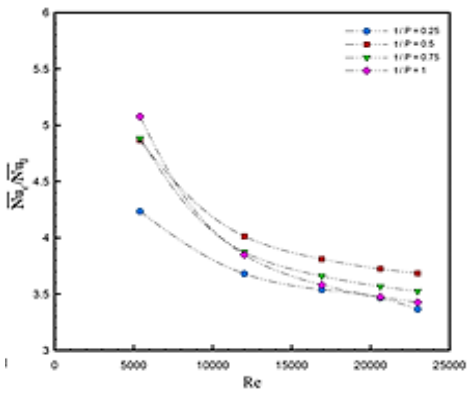

b.

Fig. 8. Variation of Nusselt number with Reynolds number for different t/P ratios; a. average Nusselt number in the roughened channel, b. ratio of average Nusselt number in the roughened channel to that of the smooth channel.

Fig. 9 shows the distribution of temperatures inside the channel at Re = 16920 for t/P = 0.25 and t/P = 0.75. The analysis of contour plots proves that the effect of t/P greatly affects the process of thermal diffusion from the roughened surface to the fluid. In the case of t/P = 0.75, there is greater heat penetration into the main flow, and there seems to be better mixing of the fluid than in the case of t/P = 0.25. Thus, heat transfer from the heated surface to the flow becomes better.

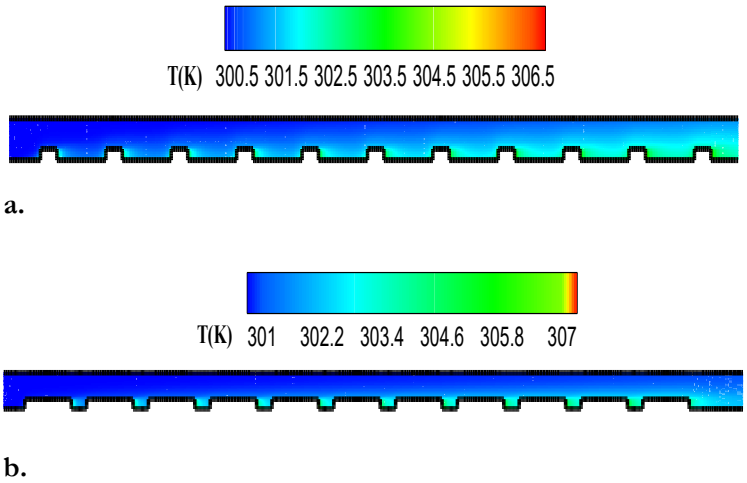

Fig. 9. Temperature distribution at Re=16920, a. t/P=0.25, b. t/P=0.75.

Fig. 10 shows the effect of Reynolds number on the value of η for various t/P ratios. It can be seen that an increase in Reynolds number causes a reduction in the value of η in all t/P ratios. It is worth mentioning that the highest value of η is attained for t/P=1.00 through the whole range of Reynolds number. Such an observation clearly demonstrates that even though improved heat transfer is one of the advantages of artificial roughness, its adverse effect on pressure drop must also be taken into consideration while evaluating the performance.

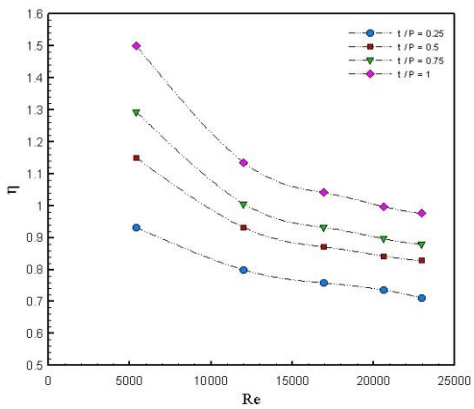

Fig. 10. Variation of thermal performance enhancement factor (η) with Reynolds number for different t/P ratios.

4.2 | Effect of Roughness Height-to-Channel Height Ratio (e/H)

In this section, the effects of roughness height to channel height ratio (e/H) on hydrodynamic and thermal properties such as friction factor, mean Nusselt number, and thermal efficiency improvement factor of the flow are studied over the mentioned Reynolds number range. In this regard, the channel geometry with a constant ratio of t/P=0.75 and four e/H ratios of 0.06, 0.13, 0.20, and 0.26 which corresponds to roughness heights of 2e=2, 4, 6, and 8 mm, respectively are investigated.

Fig. 11 shows the effect of the friction factor in the roughened channel as well as its ratio to that of the smooth channel (f/f0) versus Reynolds number for different e/H ratios. As can be seen, the friction factor increases with the increasing roughness height. This is due to the greater blocking of the flow, more flow separation, and the creation of stronger recirculating zones near roughness elements. Besides, due to increasing e/H, more surface area is available to the impinging flow and hence higher drag forces are produced which results in larger wall shear stress.

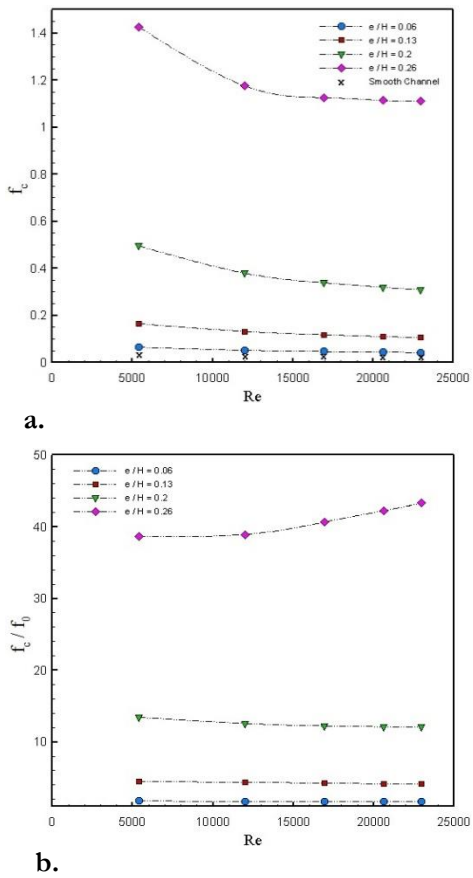

Fig. 11. Variation with Reynolds number for different e/H ratios; a. friction factor in the roughened channel, b. ratio of friction factor in the roughened channel to that of the smooth channel.

Fig. 12 depicts the streamline pattern in the roughened channel at Re=16920 for two cases, e/H=0.26 and e/H=0.13. As can be seen from *Fig. 12*, a comparison between the two geometries indicates that an increase in the roughness height causes the flow separation to be more prominent, resulting in an increase in the size and strength of the recirculation zones formed inside the cavities. For the e/H=0.26 case, the taller roughness causes more flow resistance and thus creates a complex flow structure and larger recirculation zones next to the walls.

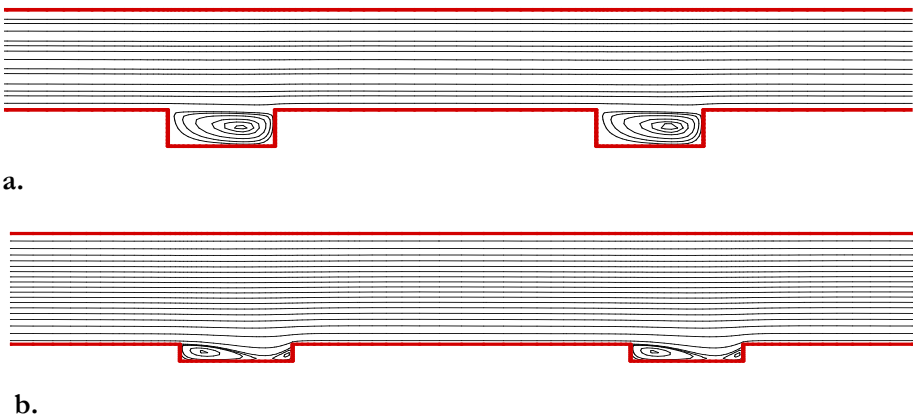

Fig. 12. Streamlines at Re=16920; a. e/H=0.26, b. e/H=0.13.

Fig. 13 shows the TKE distributions in the inter roughness regions at Re=16920 for two cases, e/H=0.26 and e/H=0.13. An increase in the roughness height causes the turbulence intensity near the walls and in the vicinity of roughness elements to become stronger. Since the taller roughness causes disturbance to the boundary layer and increases the mixing rate, the turbulence intensity is higher in the near wall regions. Higher

turbulence intensity results in higher heat transfer and higher pressure drop/friction factor. Thus, selection of proper roughness height should be made wisely in order to achieve a compromise between these two competing factors.

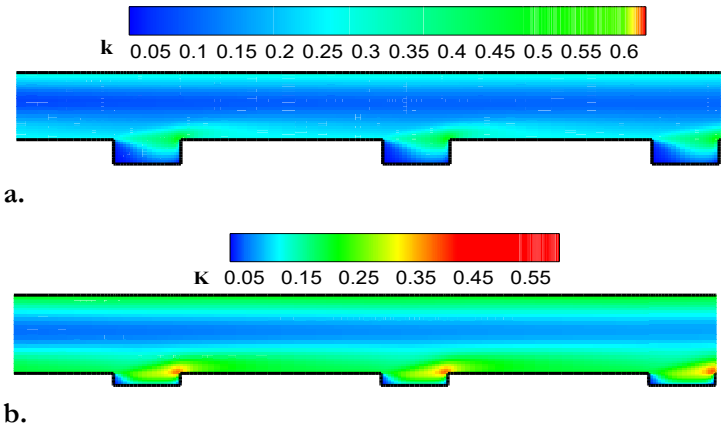

Fig. 13. TKE distribution at Re=16920; a. e/H=0.26, b. e/H=0.13.

Fig. 14 demonstrates the variation of the average Nusselt number as well as its ratio to the Nusselt number of the smooth channel (Nu/Nu0) with Reynolds number for various values of e/H. As is observed, the average Nusselt number varies almost linearly with increasing Reynolds number in all cases. What is more, with an increase in the value of e/H there occurs a substantial growth in both the Nusselt number and the Nu/Nu0 ratio. In particular, according to the experimental data obtained, the increase in the e/H ratio from 0.13 to 0.26 causes an approximately 46% increase in the average Nusselt number. Such a phenomenon is explained by turbulence intensification, mixing, thermal boundary layer thinning, and improvement in energy transfer from the heated wall to the central part of the channel.

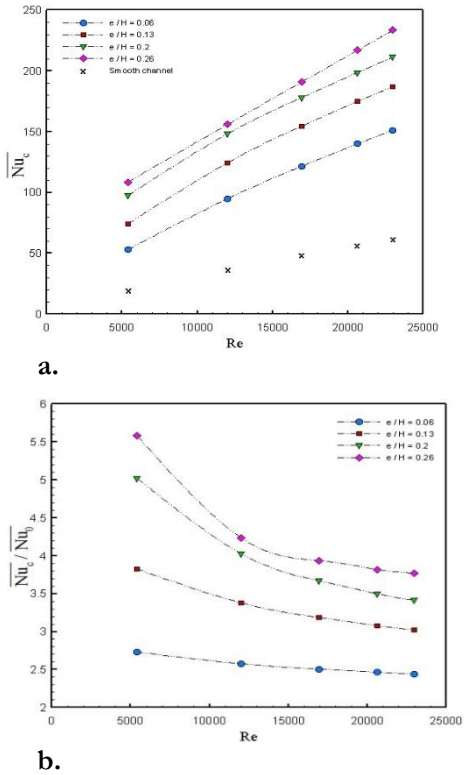

Fig. 14. Variation of Nusselt number with Reynolds number for different e/H ratios; a. average Nusselt number in the roughened channel, b. ratio of average Nusselt number in the roughened channel to that of the smooth channel.

Fig. 15 represents the temperature profiles for Re=16920 corresponding to two values of the ratio e/H=0.26 and e/H=0.13. It can be seen that the increase in the value of e/H leads to turbulence and mixing enhancement; therefore, the efficiency of heat transfer from the wall into the core of the flow is enhanced. These processes are especially characteristic for areas inside and around the roughness elements because of vortex formation facilitating energy exchange between the near-wall region and the core of the flow. Thus, the increase in e/H not only increases mixing but also provides better conditions for the heat transfer from the wall into the fluid.

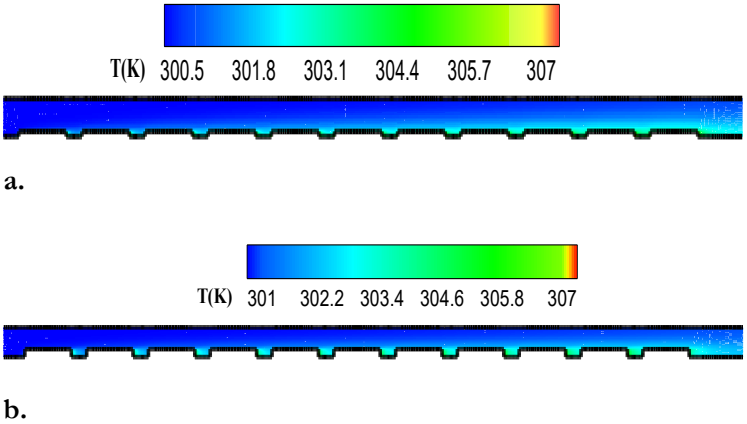

Fig. 15. Temperature distribution at Re=16920; a. e/H=0.26, b. e/H=0.13.

Fig. 6 depicts the relationship between the thermal performance enhancement factor (η) and Reynolds number for varying e/He/H. Unlike the case for the Nusselt number, an increase in the roughness height does not necessarily result in better thermo-hydraulic performance. Although the flow with the highest heat transfer efficiency is that with e/H=0.26, the substantial increase in friction factor and pressure drop results in a decrease in the thermal performance enhancement factor for this geometry. However, the flow with e/H=0.06, although offering a lower heat transfer efficiency, offers the highest value of η because of lower hydrodynamic resistance. The analysis emphasizes that in designing roughened channels, both heat transfer and pressure drop should be considered; otherwise, a higher roughness height can be detrimental to the efficiency.

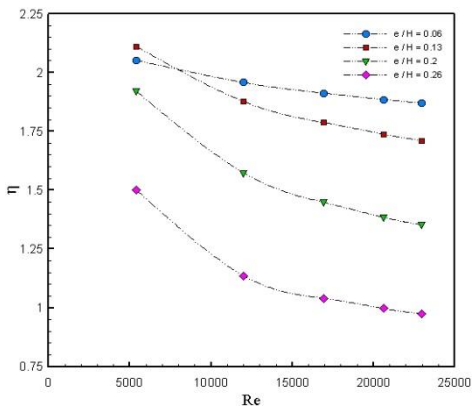

Fig. 16. Variation of thermal performance enhancement factor (η) with Reynolds number for different e/H ratios.

5 | Conclusion

In this study, a numerical investigation was carried out in detail to examine the impact of geometrical characteristics of the artificial roughness on hydrodynamics and thermodynamics performance of a rectangular channel for turbulent flow regimes. The major results obtained are presented below:

I. The effect of thickness to pitch ratio (t/P): Increasing the ratio of thickness to pitch causes decrease in the friction factor and friction factor ratio (f/f0) owing to decreasing the length of the cavity and weak

recirculation zones. Nevertheless, average Nusselt number firstly increases when increasing t/P up to 0. after which it decreases with higher values. Geometry with t/P = 1.0 provides the highest value of thermal performance enhancement factor (η) at all Re numbers.

II. Influence of ratio e/H: The significant increase in the value of the average Nusselt number can be seen by raising the value of roughness height e to 0.26 times higher than that of the channel height H, which can increase the value of the average Nusselt number by 46%. This increase may be due to an increase in turbulence and mixing as well as thinning of the thermal boundary layer. However, there is also an increase in the friction factor and pressure drop.

III. General performance trends: As Reynolds number increases, heat transfer improves in absolute terms but worsens relatively in comparison with that in a smooth channel. It is shown by decreasing trends of Nu/Nu0 and η. Thus, a joint consideration of thermal and hydraulic performance of roughened channels is essential in their design.

IV. Design implications: An optimum choice of roughness geometrical parameters should be a compromise between increase of heat transfer and rise of flow resistance. In the present case, t/P=1.00t/P=1.00 and e/H=0.06e/H=0.06 lead to the best thermo hydraulic performance of roughened channels. This information could be used by engineers in design of compact heat exchangers, gas turbine cooling channels, and other heat transfer equipment.

Funding

No funding was received for conducting this study.

Data Availability

All data are included in the text.

Conflicts of Interest

The authors declare no competing interests.

Reference

[1] Bergles, A. E. (2002). ExHFT for fourth generation heat transfer technology. *Experimental thermal and fluid science*, *26*(2), 335–344. https://doi.org/10.1016/S0894-1777(02)00145-0

[2] Webb, R. L., & Kim, N. H. (2004). *Principles enhanced heat trans*. Garland Science. https://doi.org/10.1201/b12413

[3] Zhou, F., & Catton, I. (2013). A numerical investigation of turbulent flow and heat transfer in rectangular channels with elliptic scale-roughened walls. *Journal of heat transfer*, *135*(8), 81901. https://doi.org/10.1115/1.4024278

[4] Singh, I., & Singh, S. (2018). A review of artificial roughness geometries employed in solar air heaters. *Renewable and sustainable energy reviews*, *92*, 405–425. https://doi.org/10.1016/j.rser.2018.04.108

[5] Burns, J. C., & Parkes, T. (1967). Peristaltic motion. *Journal of fluid mechanics*, *29*(4), 731–743. 10.1017/S0022112067001156

[6] Goldstein Leonardo, J., & Sparrow, E. M. (1977). Heat/Mass transfer characteristics for flow in a corrugated wall channel. *Journal of heat transfer*, *99*(2), 187–195. https://doi.org/10.1115/1.3450667

[7] O'Brien, J. E., & Sparrow, E. M. (1982). Corrugated-duct heat transfer, pressure drop, and flow visualization. *Journal of heat transfer*, *104*(3), 410–416. https://doi.org/10.1115/1.3245108

[8] Saniei, N., & Dini, S. (1993). Heat Transfer Characteristics in a Wavy-Walled Channel. *Journal of heat transfer*, *115*(3), 788–792. https://doi.org/10.1115/1.2910756

[9] Wang, G., & Vanka, S. P. (1995). Convective heat transfer in periodic wavy passages. *International journal of heat and mass transfer*, *38*(17), 3219–3230. https://doi.org/10.1016/0017-9310(95)00051-A

[10] Patel, V. C., Chon, J. T., & Yoon, J. Y. (1991). Turbulent flow in a channel with a wavy wall. *Journal of fluids engineering*, *113*(4), 579–586. https://doi.org/10.1115/1.2926518

[11] Gloerfelt, X., & Cinnella, P. (2019). Large eddy simulation requirements for the flow over periodic hills. *Flow, turbulence and combustion*, *103*(1), 55–91. https://doi.org/10.1007/s10494-018-0005-5

[12] Ziefle, J., Stolz, S., & Kleiser, L. (2008). Large-eddy simulation of separated flow in a channel with streamwise-periodic constrictions. *AIAA journal*, *46*(7), 1705–1718. https://doi.org/10.2514/1.33891

[13] Yang, L. C., Asako, Y., Yamaguchi, Y., & Faghri, M. (1997). Numerical prediction of transitional characteristics of flow and heat transfer in a corrugated duct. *Journal of heat transfer*, *119*(1), 62–69. https://doi.org/10.1115/1.2824101

[14] Amano, R. S. (1985). A numerical study of laminar and turbulent heat transfer in a periodically corrugated wall channel. *Journal of heat transfer*, *107*(3), 564–569. https://doi.org/10.1115/1.3247461

[15] Islamoglu, Y., & Parmaksizoglu, C. (2003). The effect of channel height on the enhanced heat transfer characteristics in a corrugated heat exchanger channel. *Applied thermal engineering*, *23*(8), 979–987. https://doi.org/10.1016/S1359-4311(03)00029-2

[16] Islamoglu, Y., & Parmaksizoglu, C. (2004). Numerical investigation of convective heat transfer and pressure drop in a corrugated heat exchanger channel. *Applied thermal engineering*, *24*(1), 141–147. https://doi.org/10.1016/j.applthermaleng.2003.07.004

[17] Naphon, P. (2007). Heat transfer characteristics and pressure drop in channel with V corrugated upper and lower plates. *Energy conversion and management*, *48*(5), 1516–1524. https://doi.org/10.1016/j.enconman.2006.11.020

[18] Naphon, P., & Kornkumjayrit, K. (2008). Numerical analysis on the fluid flow and heat transfer in the channel with V-shaped wavy lower plate. *International communications in heat and mass transfer*, *35*(7), 839–843. https://doi.org/10.1016/j.icheatmasstransfer.2008.03.010

[19] Naphon, P. (2008). Effect of corrugated plates in an in-phase arrangement on the heat transfer and flow developments. *International journal of heat and mass transfer*, *51*(15), 3963–3971. https://doi.org/10.1016/j.ijheatmasstransfer.2007.11.050

[20] Eiamsa-ard, S., & Promvonge, P. (2008). Numerical study on heat transfer of turbulent channel flow over periodic grooves. *International communications in heat and mass transfer*, *35*(7), 844–852. https://doi.org/10.1016/j.icheatmasstransfer.2008.03.008

[21] Thianpong, C., Chompookham, T., Skullong, S., & Promvonge, P. (2009). Thermal characterization of turbulent flow in a channel with isosceles triangular ribs. *International communications in heat and mass transfer*, *36*(7), 712–717. https://doi.org/10.1016/j.icheatmasstransfer.2009.03.027

[22] Elshafei, E. A. M., Awad, M. M., El-Negiry, E., & Ali, A. G. (2010). Heat transfer and pressure drop in corrugated channels. *Energy*, *35*(1), 101–110. https://doi.org/10.1016/j.energy.2009.08.031

[23] Yin, J., Yang, G., & Li, Y. (2012). The effects of wavy plate phase shift on flow and heat transfer characteristics in corrugated channel. *Energy procedia*, *14*, 1566–1573. https://doi.org/10.1016/j.egypro.2011.12.1134

[24] Tanda, G. (2011). Effect of rib spacing on heat transfer and friction in a rectangular channel with 45° angled rib turbulators on one/two walls. *International journal of heat and mass transfer*, *54*(5), 1081–1090. https://doi.org/10.1016/j.ijheatmasstransfer.2010.11.015

[25] Ramgadia, A. G., & Saha, A. K. (2012). Fully developed flow and heat transfer characteristics in a wavy passage: Effect of amplitude of waviness and Reynolds number. *International journal of heat and mass transfer*, *55*(9), 2494–2509. https://doi.org/10.1016/j.ijheatmasstransfer.2012.01.010

[26] Desrues, T., Marty, P., & Fourmigué, J. F. (2012). Numerical prediction of heat transfer and pressure drop in three-dimensional channels with alternated opposed ribs. *Applied thermal engineering*, *45–46*, 52–63. https://doi.org/10.1016/j.applthermaleng.2012.03.013

[27] Mohammed, H. A., Abed, A. M., & Wahid, M. A. (2013). The effects of geometrical parameters of a corrugated channel with in out-of-phase arrangement. *International communications in heat and mass transfer*, *40*, 47–57. https://doi.org/10.1016/j.icheatmasstransfer.2012.10.022

[28] Ravi, B. V., Singh, P., & Ekkad, S. V. (2017). Numerical investigation of turbulent flow and heat transfer in two-pass ribbed channels. *International journal of thermal sciences*, *112*, 31–43. https://doi.org/10.1016/j.ijthermalsci.2016.09.034

[29] Versteeg, H. K., & Malalasekera, W. (2007). *An introduction to computational fluid dynamics: The finite volume method*. Pearson Education Limited. https://books.google.com/books/about/An_Introduction_to_Computational_Fluid_D.html?id=RvBZ-UMpGzIC

[30] Launder, B. E., & Spalding, D. B. (1983). Paper 8 - The numerical computation of turbulent flows. In *Numerical prediction of flow, heat transfer, turbulence and combustion* (pp. 96–116). Pergamon. https://doi.org/10.1016/B978-0-08-030937-8.50016-7

Appendix

Table A1. Symbol and definition.

Symbol	Definition	Unit
-	Heat transfer surface area	A
m	Side length of the obstacle (rib)	a
m	Hydraulic diameter	D_h
-	Friction factor	f
N/m^3	Production rate of TKE	G
$W/m^2 K$	Convective heat transfer coefficient	h
m	Channel height	H
-	Turbulence intensity	I
J	TKE	k
W/m K	Thermal conductivity	K
m	Turbulence length scale	l
m	Channel length	L
-	Nusselt number	Nu
Pa	Pressure	P
W/m^2	Wall heat flux	q''
-	Reynolds number	Re
°C	Temperature	T
m/s	Velocity component	u
m/s	Mean (bulk) velocity	U
m	Coordinate along the flow direction	X
Greek Symbols		
-	Inverse of effective Prandtl number	α
-	Turbulence model constant	β
-	Thermal diffusivity	Γ
-	Kronecker delta	δ_{ij}
1/s	Specific dissipation rate	ω
-	Thermal performance enhancement factor	η
°	Obstacle (rib) angle	θ
Pa.s	Dynamic viscosity	μ
m	Spanwise (lateral) direction	z